Preparation and Properties of $BaBiBO_4 – SiO_2$ Glasses

Reenamoni Saikia Chaliha, Anal Tarafder, K. Annapurna and Basudeb Karmakar*

Glass Science and Technology Section, Glass Division, Central Glass and Ceramic Research Institute (Council of Scientific and Industrial Research, CSIR)
196, Raja S.C. Mullick Road, Kolkata 700032, India

Abstract

Glasses in the new system (100-x) $BaBiBO_4$ – x SiO_2 where x = 10 - 50 (mol %) were prepared by the melt-quench technique. The density of the glasses increases with increase in $BaBiBO_4$ content because of its higher molecular mass. Glass transition temperature (T_g), glass deformation temperature (T_d) and glass softening point (T_s) decrease while coefficient of thermal expansion (CTE) increases with increase in $BaBiBO_4$ content. Vis-NIR spectra reveal that with increasing melting temperature transmission of the glasses decreases due to auto thermal reduction of Bi^{3+} to Bi^0 as confirmed in by TEM and SAED analyses. FTIRR spectra of the glasses indicate the formation of BiO_6, BO_3 and BO_4 structural units. Ferroelectric $BaBiBO_4$ crystalline phase is obtained from these glasses by controlled heat-treatment at 580°C. XRD analysis reveals its 45-66 nm crystallite size range. Whereas the FESEM images show the formation of polycrystalline spherical grains of 89-194 nm along with single-crystalline micro rods of average diameter of 0.5-1.5 μm and aspect ratio of 10.8-5.7 on the surface as the micro regions. Dielectric constant of the glasses increases with increase in $BaBiBO_4$ content which is attributed to the combined effects of high polarization and ionic refraction of both Bi^{3+} and Ba^{2+} ions. It is demonstrated here that $BaBiBO_4$–SiO_2 is a promising glass system for the synthesis of glass-ceramics of novel $BaBiBO_4$ nonlinear optical (NLO) crystal.

Keywords: $BaBiBO_4$ glass; Transmission; Thermal properties; Ferroelectric $BaBiBO_4$ crystals; Dielectric constant, Infrared reflection spectra.

---

*Corresponding author. Tel.: +91-33 2473 3469; fax: +91-33 2473 0957
E-mail address: basudebk@cgcri.res.in (B. Karmakar)

Introduction

Glass-ceramic systems comprising the crystalline phases of ferroelectric/electro-optic materials are widely used in various fields, such as in information technology, energy conversion, infrared detection etc., because of their excellent piezoelectric, dielectric, pyroelectric and nonlinear optical (NLO) properties.[1-4] Recently, there has been an increasing interest in the synthesis, structure and physical properties of heavy metal oxide glasses containing Bi_2O_3 due to their high refractive index, high infrared transparency and increased third order nonlinear optical susceptibility.[5] It is well known that barium containing crystals (β-BaB_2O_4 or β-BBO) are important materials for nonlinear optical applications in the visible and ultraviolet regions.[6] In addition to barium borate, bismuth containing borate crystals have received great attention due to their interesting nonlinear optical, piezoelectric and luminescent properties for technical applications. Over and above Bi_2O_3 and BaO are in the interest for replacing lead oxide in PbO-B_2O_3-SiO_2 glass system in quest of environmental friendly NLO materials.[7] In the binary bismuth borate system, the crystalline bismuth compounds studied are $Bi_{24}B_2O_{39}$, $Bi_4B_2O_9$, $Bi_3B_5O_{12}$, α-, β- and γ-BiB_3O_6, $BiBO_3$ and $Bi_2B_8O_{15}$.[8] The crystal structures $Ba_5(BO_3)_2(B_2O_5)$, BaB_2O_4, BaB_4O_7, $Ba_2B_{10}O_{17}$ and BaB_8O_{13} have also been reported in the BaO-B_2O_3 system.[8]

The $BaBiBO_4$ crystal was discovered by Barbier et al.[9] in 2005. They have also reported that its efficiency for second harmonic generation (SHG) is about five times more than that of KH_2PO_4 (KDP). The NLO property of $BaBiBO_4$ is due to its non-centrosymmetric crystal structures. Thus, the $BaBiBO_4$–SiO_2 glass system is of special interest for the reason that it results in $BaBiBO_4$[9] crystal containing glass-ceramics on

controlled heat-treatment. However, $BaBiBO_4$ alone does not form glass. For this reason, its glass formation is ensured by adding a well known glass former, silicon dioxide (SiO_2). Various researchers have reported different glass systems for creation of NLO crystals in glass-ceramics.[2-5,7] Recently, we have reported dielectric, structural and luminescent properties of rare earth doped NLO $KNbO_3$ and $LiTaO_3$ crystals in the silicate glass systems.[10-12] As we aware, glass formation and its subsequent conversion into $BaBiBO_4$ crystal containing glass-ceramics in the $BaBiBO_4$–SiO_2 glass system have not been reported so far.

In view of above, in this paper we report the structural, dielectric, optical and thermal properties of the glasses in the $BaBiBO_4$–SiO_2 system. The glasses and glass-ceramics have been studied by differential thermal analysis (DTA), dilatometry, X-ray diffraction (XRD), field emission scanning electron microscopy (FESEM), transmission electron microscopy (TEM) and Fourier transform infrared reflection spectroscopy (FTIRRS).

Experimental Procedure

Preparation of Glass

Glasses of composition (mol %) (100-x) $BaBiBO_4$ – x SiO_2 (where x = 10, 15, 20, 30, 40 and 50, and $BaBiBO_4$ is 50BaO-25Bi_2O_3-25B_2O_3) were prepared using high purity $BaCO_3$ (GR, 99%, Fluka), Bi_2O_3 (GR, 99.9%, Aldrich), H_3BO_3 (GR, 99.5%, Fluka) and SiO_2 (99.99%) as raw materials by the melt-quench technique. 100 g glass was melted in a platinum crucible in an electrically heated furnance at 1050, 1150, 1200 and 1250°C for 1.5 h. Lower melting temperature is preferable for high $BaBiBO_4$ content glasses with

respect to reduce loss of B_2O_3 component and to ensure high transparency. Nominal glass composition, melting temperature and some properties of the glasses are listed in Table I. The melts were homogenized by intermittent stirring and followed by pouring onto a pre-heated iron mould. In order to remove the internal stresses the glass block were subsequently annealed at 420^oC for 2 h. The as-prepared glass blocks were cut into desired dimensions and polished for undertaking different measurements. The as-prepared glasses were labeled as B1, B2, B3a, B3b, B3c, B4, B5 and B6 respectively for convenience.

Characterization Techniques

The densities of the as-prepared glasses were measured by following the standard Archimedes' principle using distilled water as the buoyancy liquid. The refractive indices of the glasses at five different wavelengths (473, 532, 632.8, 1064 and 1552 nm) were measured by a prism coupling measurement technique (Model Metricon 2010/M). The DTA curves were recorded on a Netzsch STA 409 C/CD instrument from room temperature to 1000^oC at a heating rate of 10^oC/min. Glass transition temperature (T_g), co-efficient of thermal expansion (CTE) and glass deformation temperature (T_d) of the as-prepared glass samples were evaluated using a horizontal dilatometer (model DIL 402 PC, Netzsch-Gerätebau GmbH, Germany). Softening temperature (T_s) was measured using a glass softening point system (Model SP-3A, Harrop Industries Inc., OH, USA).

The optical transmission spectra of the polished glasses were recorded in the wavelength range of 400-1100 nm with an accuracy of ±1%, using a double beam UV-Vis-NIR spectrophotometer (Model Lambda 20, Perkin-Elmer Corporation, Waltham,

MA, USA). The FTIR reflectance spectra were traced using a FTIR spectrometer (Model 1615, Perkin Elmer Corporation, Waltham, MA, USA) in the wave number range of 400–2000 cm^{-1} with a spectral resolution of $\pm$ 2 cm^{-1} and at a 15^{o} angle of incidence after 16 scans. Powder X-ray diffraction (XRD) patterns were recorded using an Xpert-Pro MPD diffractometer (PANalytical, Almelo, The Netherlands) (CuKα) with nickel filtered and anchor scan parameters wavelength of 1.5406 Å at 25^{o}C having the source power of 40 kV and 30 mA to confirm the amorphous nature of the as-prepared samples and for the phase identification in the crystallized samples. The morphology of the heat-treated glasses was examined by FESEM. A Carl Zeiss high resolution field emission electron microscope (FESEM) (model SUPRA 35 VP) with the parameters gun vacuum = 3×10^{-10} mbar, system vacuum = 2.65×10^{-5} mbar and extractor current = 159.3 μA for FESEM measurement. Freshly fractured surfaces of the heat-treated glasses were etched in 2% HF solution for 2 min and were coated with a thin carbon film for the above measurements. And the TEM and selected area electron diffraction (SAED) of the powdered glass–ceramic sample were done on an FEI (Model Tecnai G^2 30ST, FEI Company, and Hillsboro, OR) instrument. The dielectric constant of all the samples was measured at room temperature using a Hioki LCR meter (Model: 3532-50 LCR Hitester, Hioki, Ueda, Nagano, Japan) at 1 MHz frequency after coating the surfaces with a conductive silver paint followed by drying at 140^{0}C for 1 h.

Results and Discussion

Physical and Thermal Properties

The nominal chemical composition, melting temperature and color of the glasses are given in Table 1. Chemical analysis has revealed that the loss of B_2O_3 component of the glass due to evaporation at the melting temperature varies in the range 1-3 mol% which increases with increase in $BaBiBO_4$ content and melting temperature. The densities of the glasses are found to be varied between 4.93-6.10 $g.cm^{-3}$ and their plot against $BaBiBO_4$ content in the glass matrix is shown in Fig. 1. The density of the glasses increases with increase in $BaBiBO_4$ content due to its higher atomic weights of barium and bismuth.[13,14] The measured refractive indices of all the glasses at 473, 532, 632.8, 1060 and 1552 nm were fitted with the Cauchy dispersion fitting to obtain the refractive indices at standard wavelengths, n_e (λ = 546.1 nm), $n_{F'}$ (λ = 480 nm) and $n_{C'}$ (λ = 643.8 nm). From the measured glass density, refractive indices (n_e, $n_{F'}$ and $n_{C'}$) at three different wavelengths and other related optical properties have been determined using relevant expressions, and the results are presented in Table II. The variation of refractive index of the as-prepared glasses as a function of wavelength is shown in Fig. 2. Refractive indices were found to increase with increase in $BaBiBO_4$ content in the glasses and decrease with increase in wavelength of light. This sharp variation in refractive indices with increasing $BaBiBO_4$ content in the glasses occurs mainly because of the more dense structure of the glass and also due to the incorporation of more polarisable (Ba = 4.67 $Å^3$, Bi = 1.31 $Å^3$) as well as more ionic refraction (Ba = 16.8 cm^3, Bi = 30.5 cm^3) of Ba and Bi ions.[15] For the same reason, the value of molar refractivity (R_M) and electronic polarizability (α) increases with increase in $BaBiBO_4$ content in the glasses.

Figure 3 shows the representative DTA curves of B1 and B3b glasses. The DTA curve of B1 glass exhibits an inflection in the temperature range 401-425^{o}C followed by an exothermic peak at 519^{o}C (T_p) and the same of B3b glass exhibits an inflection in the temperature range 407-459^{o}C followed by an exothermic peak at 583^{o}C (T_p) corresponding to the phase crystallization. The point of intersection of the tangents drawn at the slope change as marked in Fig. 3 of the DTA curves estimates the glass transition temperature (T_g) for B1 glass to be 416 and for B3b glass to be 440^{o}C. From the DTA data, the glass thermal stability factor ($\Delta = T_p - T_g$) has been determined and found to be 103 for B1 and 143^{o}C for B3b glasses respectively. Reasonably, high glass stability factor specifies the ability of this glass in forming nano-structured glass-ceramic under controlled heat-treatment. From the DTA curves it is seen that the glass transition and crystallization peak temperature increases to the higher temperature with decreasing $BaBiBO_4$ content. This is also confirmed by the dilatometric measurements. Some selected curves of such measurements are shown in Fig. 4 to show the method of determination of T_g, T_d and CTE properties of the glasses. The variation of glass transition (T_g), glass deformation (T_d) and softening temperature (T_s) with increase of $BaBiBO_4$ content in the glass matrix is shown in Fig. 5. As the T_g is reduced with increase in $BaBiBO_4$ content, the similar trends may also be expected for deformation temperature (T_d) as well as softening temperature (T_s). These are due to the lower melting temperature of Bi_2O_3 (824^{o}C) than that of SiO_2 (1723^{o}C). But the coefficient of thermal expansion (CTE) increases with increase of $BaBiBO_4$ content in the glass matrix as shown in Fig. 6. The reason is that with increase of BaO and Bi_2O_3 content the rigidity of the glasses decrease due to the formation of non-bridging oxygen and thereby the thermal

expansion increases.[7,16-19] In addition to these, the SiO_2 component has very low CTE (5.5×10^{-7} K^{-1}) compared to $BaBiBO_4$ component. Being CTE an additive property of the constituents of a glass, hence the increase of CTE with increase in $BaBiBO_4$ content.

Transmission Spectra

Visible-near infrared (NIR) transmission spectra of the B3a, B3b and B3c glasses melted at 1050, 1150 and 1250°C respectively and B4 glass melted at 1200°C in the wavelength range of 400-1100 nm are shown in Fig. 7. From the transmission spectra it is seen that with increasing the melting temperature of the glass, transmission of the glass decreases remarkably. Gerth and Russel[14,20] also observed that the color of the samples changes from yellow to brown depending on the composition and melting temperatures. They reported that samples possessing higher Bi_2O_3 concentrations are more intensely colored if melted at the same temperatures. The effect of melting temperature is caused by a partial auto thermo reduction to metallic bismuth (Bi^0) of Bi_2O_3. With increase in melting temperature the redox equilibrium according to the Eq. (1) is shifted to the right side.[21]

$$Bi_2O_3 \leftrightarrow 2Bi^0 + 3/2\ O_2 \qquad (1)$$

To verify this fact SAED and HRTEM images were examined during TEM studies. Diffraction from the SAED image and the lattice planes formed in the HRTEM images shows the presence of rhombohedral Bi^0. The details of this study are provided in section of FESEM and TEM analyses. From the spectra shown in Fig. 7, it may be considered that the glass melting temperature 1100°C is optimum for this system with respect to the optical transmission point of view.

FTIR Reflection Spectra

The FTIR reflectance spectra of the glasses in the wavenumber range of 400–2000 cm^{-1} are shown in Fig. 8. The peak at 486 cm^{-1} in B1 glass shifted to lower wavenumber side as the $BaBiBO_4$ content decreases and reaches at 438 cm^{-1} in B6 glass. The intensity of this peak increases as the $BaBiBO_4$ content decreases in the glass matrix. This peak is attributed to the various modes of Bi-O-Bi vibration in BiO_6 octahedra.[13,16,22] The bond bending vibration of B-O-B linkages of the boron-oxygen network between two trigonal boron atoms in BO_3 triangles appear in the FTIRR spectra between 690 and 715 cm^{-1} for B1 to B6 glasses.[13,23] The peak at 868 cm^{-1} in B1 glass shifted to 903 cm^{-1} in B5 glass is due to the stretching vibrations of BO_4 units which are connected by the bismuth cations.[13] The peak 957 cm^{-1} in B6 glass which grows with increase in SiO_2 content is attributed to the Si-O stretching in SiO_4 tetrahedral units with non-bridging oxygen atoms. B-O stretching of tetrahedral BO_4^- units appear in the B1 glass at 1108 cm^{-1} and in the B5 glass at 1197 cm^{-1}.[24] The peak at 1265 cm^{-1} in B1 and at 1320 cm^{-1} in B6 glasses is due to B-O stretching vibrations of trigonal BO_3 units.[13,24] The peaks at 868, 1108 and 1265 cm^{-1} in B1 glass shifted to higher wavenumber side and the intensity of the peaks decreases as the amount of $BaBiBO_4$ in the glass phase decreases. These are the evidences of presence of borate superstructural units throughout the glass formation range. The band below 500 cm^{-1} is due to the BiO_6 groups.

XRD Analysis

Figure 9 shows the XRD patterns of as-prepared glass B3b and heat-treated glasses B2 and B3b at 580°C for 2 h. The XRD patterns of all the as-prepared glasses

follow the same characteristics as shown in Fig. 9. They exhibit a broad peak around 2θ = 28°, which confirm their amorphous nature. After heat-treatment all the samples are found to be surface crystallized. The major crystalline phase formed is identified as $BaBiBO_4$, which is in accordance to Barbier et al.[9] Some of the low intense peaks in the XRD patterns are identified as the formation of metallic Bi^0 in accordance to the JCPDS file cards 85-1331, 85-1329 and 26-0214 of known metallic Bi^0. From the full width at half maximum (FWHM) of the intense diffraction peak of $BaBiBO_4$, the average crystallite size (diameter, d) is calculated by using Scherrer's formula,[25]

$$d = 0.9\,\lambda/\beta\cos\theta \qquad (2)$$

where λ is the wavelength of X-ray radiation (CuKα = 1.5406 Å) and β is the full-width at half-maximum (FWHM) of the peak at 2θ. The average crystallite size was found to vary in the range of 45-66 nm for samples B2 and B3b.

FESEM and TEM Analyses

Figures 10 (a), (b) and (c) depict the FESEM micrographs of surface crystallization and Fig. 10 (d) bulk crystallization of B3b glass-ceramics heat-treated at 580°C for 2 h. During heat-treatment $BaBiBO_4$ single-crystalline micro rods were grown on the surface of the glass-ceramics as micro region (Fig. 10 (a) and (b)). The diameter and length of the micro rods are found to be varying in the ranges 0.5-1.5 and 5.4-8.6 μm respectively, and the aspect ratio in the range 10.8-5.7. The micrographs in Fig. 10 (c) and (d) show polycrystalline grains of almost uniform size are homogeneously dispersed in the glassy matrix. Analyzing Fig. 10 (a)-(c), it is clear that the granular polycrystals are merged with one another yielding the micro rods. From the XRD analysis it is found that

the crystallite sizes are in the range 45-66 nm, whereas FESEM micrograph shows that spherical grains of sizes 89-194 nm are formed. From this fact it may be ascertained that the glass-ceramics developed in the present investigation are polycrystalline in nature.

The bright field TEM images of B4 and B3c glasses along with respective SAED image are shown in Fig 11 (a and b) and (c) respectively. The nano particle nature of the material is confirmed from the diffused hallow of SAED image obtained from the glass. Fig. 11 (a) reveals that black particles of diameter about 6 nm shown in image are due to the formation of Bi^0 metallic particles. These metallic particles are formed due to the auto thermo reduction reaction (see Eq. 1, discussed earlier) took place at melting temperature $\geq$ 1050 °C. The (hkl) plane <024> obtained from the pattern are matching with the rhombohedral Bi^0 (JCPDS file no. 85-1331) are indicated in the image (Fig. 11 (c)). From the HRTEM image (Fig. 11 (d)), the atomic or lattice fringes of formed Bi^0 have been clearly observed and the distance between any two planes is found to be 3.33 Å. The formed lattice planes from the HRTEM image resemble well with the d-spacing of the planes as reported in the JCPDS card file no. 85-1331 of known bismuth metal. Thus, the TEM image reveals the presence of nano particles of metallic bismuth in the glass. Figure 11 (b) shows the formation of smaller bismuth nano particles in glass B4 which contains lower amount of $BaBiBO_4$ compared to B3c and lower melting temperature as well.

Dielectric Constant

The variation of the dielectric constant of the glasses with increase of $BaBiBO_4$ content is shown in Fig. 12. The as-prepared glasses exhibit a relatively higher values of dielectric constant (ε = 16-23) than that of the normal glasses such as vitreous silica (ε =

3.8), soda-lime silicate (ε = 7-10)[26-28] or borosilicate glasses (ε = 4.5-8).[26,29,30] It is seen that with increase in Bi_2O_3 and BaO contents in the glass the dielectric constant increases. This is due to the very high ionic refraction (Bi = 30.5 cm^3 and Ba = 16.8 cm^3) and polarizability (Bi = 1.31 $Å^3$ and Ba = 4.67 $Å^3$) of Bi^{3+} and Ba^{2+} ions present in the material as discussed earlier.[15] It is also due to spontaneous polarization of Bi^{3+} ion under applied electric field having one lone pair of s-electron in the electronic configuration ($5d^{10}6s^26p^0$). This lone pair promotes pyramidal bonding and the structural unit possesses high dipole moment which results in spontaneous polarization[14].

Conclusions

Various properties of the glasses in the system (100-x) $BaBiBO_4$ – x SiO_2 (where x = 10 - 50 and $BaBiBO_4$ is 50BaO-25Bi_2O_3-25B_2O_3 (mol %)) were investigated in this study. With increase in $BaBiBO_4$ content in the glass the density and thermal expansion co-efficient (α) increase, but glass transition temperature (T_g), deformation temperature (T_d) and softening temperature (T_s) decrease monotonically. Due to the presence of Bi_2O_3 where Bi has a very high ionic refraction as well as polarizability the refractive index increases. The study on the effect of melting temperatures on the transparency of the glasses revealed that for this present glass system 1100°C melting temperature gives the optimum transparency. The darkening of the glass color with increasing melting temperature and $BaBiBO_4$ content is also evident due to a partial auto thermo reduction of Bi^{3+} ion to metallic bismuth Bi^0. XRD studies confirm the presence of ferroelectric $BaBiBO_4$ crystalline phase in the heat-treated glasses. Granular polycrystals of 89-194 nm and also micro rods of average diameter of 0.5-1.5 μm are developed during

cryatallization of glasses as revealed in the microstructural studies. Dielectric constant of the as-prepared glasses increases with increase of Bi_2O_3 and BaO content which is attributed to the combined effects of high polarization and ionic refraction of Bi^{3+} and also high polarizability of Ba^{2+} ion. It is demonstrated that $BaBiBO_4$–SiO_2 is a promising glass system for the synthesis of glass-ceramics containing novel $BaBiBO_4$ ferroelectric crystal.

Acknowledgements

This research work was supported by BRNS/DAE under the sanction No. 2007/34/05-BRNS. The authors gratefully thank Dr. H. S. Maiti, Director of the institute for his kind permission to publish this paper. The technical supports provided by the infrastructural facility (X-ray and Electron Microscopy Divisions) of this institute for recording XRD and TEM image are also thankfully acknowledged.

References

1. X. Jin, D. Sun, M. Zhang, Y. Zhu, and J. Qian, "Investigation on FTIR spectra of barium calcium titanate ceramics," *J. Electroceram.,* **22** 285-290 (2009).
2. M. V. Shankar and K. B. R. Varma, "Crystallization, dielectric and optical studies on strontium tetraborate glasses containing bismuth titanate," *Mater. Res. Bull.,* **33** 1769-1782 (1998).
3. K. B. R. Varma, M. V. Shankar, and G. N. Subbanna, "Structural and dielectric characteristics of strontium tetraborate-bismuth vanadate glass-ceramics," *Mater. Res. Bull.*, **31** 475-482 (1996).
4. G. S. Murugan and K. B. R. Varma, "Structural, dielectric and optical properties of lithium borate-bismuth tungstate glass-ceramics," *Mater. Res. Bull.*, **34** 2201-2213. (1999)
5. C. E. Stone, A. C. Wright, R. N. Sinclair, S. A. Feller, M. Affatigato, D. L. Hogan, N. D. Nelson, C. Vira, Y. B. Dimitriev, E. M. Gattef, and D. Ehrt, "Structure of bismuth borate glasses," *Phys. Chem. Glasses*, **41** 409-412 (2000).
6. L. J. Q. Maia, M. I. B. Bernardi, A. R. Zanatta, A. C. Hernandes, and V. R. Mastelaro, "β-BaB_2O_4 nanometric powder obtained from the ternary BaO-B_2O_3-TiO_2 system using the polymeric precursor method," *Mater. Sci. Eng. B*, **107** 33-38 (2004).
7. B-S. Kim, E-S. Lim, J-H. Lee, and J-J. Kim, "Effect of Bi_2O_3 content on sintering and crystallization behavior of low-temperature firing Bi_2O_3-B_2O_3-SiO_2 glasses," *J. Eur. Ceram. Soc.*, **27** 819-824 (2007).
8. R. S. Bubnova, S. V. Krivovichev, S. K. Filatov, A. V. Egorysheva, and Y. F. Kargin, "Preparation, crystal structure and thermal expansion of a new bismuth barium borate,

$BaBi_2B_4O_{10,}$" *J. Solid State Chem.,* **180** 596-603 (2007).

9. J. Barbier, N. Penin, A. Denoyer, and L. M. D. Cranswick, "$BaBiBO_4$, a novel non-centrosymmetric borate oxide," *Solid State Sci.*, **7** 1055-1061 (2005).
10. R. S. Chaliha, K. Annapurna, A. Tarafder, V. S. Tiwari, P. K. Gupta, and B. Karmakar, "Luminescence and dielectric properties of nano-structured Eu^{3+}:K_2O–Nb_2O_5–SiO_2 glass-ceramics," *Solid State Sci.*, **11** 1325-1332 (2009).
11. A. Tarafder, K. Annapurna, R. S. Chaliha, V. S. Tiwari, P. K. Gupta, and B. Karmakar, "Processing and Properties of Eu^{3+}:$LiTaO_3$ Transparent Glass–Ceramic Nanocomposites," *J. Am. Ceram. Soc.,* **92** 1934–1939 (2009).
12. A. Tarafder, K. Annapurna, R. S. Chaliha, V. S. Tiwari, P. K. Gupta, and B. Karmakar, "Nanostructuring and fluorescence properties of Eu^{3+}:$LiTaO_3$ in Li_2O–Ta_2O_5–SiO_2–Al_2O_3 glass-ceramics," *J Mater. Sci.,* **44** 4495–4498 (2009).
13. H. Doweidar and Y. B. Saddeek, "FTIR and ultrasonic investigations on modified bismuth borate glasses," *J. Non-Cryst. Solids,* **355** 348-354 (2009).
14. K. Gerth and C. Rüssel, "Crystallization of $Bi_4Ti_3O_{12}$ from glasses in the system Bi_2O_3/TiO_2/$B_2O_{3,}$" *J. Non-Cryst. Solids,* **221** 10-17 (1997).
15. M. B. Volf, *Chemical Approach to Glass,* pp. 118-131, Elsevier, Amsterdam-Oxford-New York-Tokyo, 1984.
16. D. Saritha, Y. Markandeya, M. Salagram, M. Vithal, A. K. Singh, and G. Bhikshamaiah, "Effect of Bi_2O_3 on physical, optical and structural studies of ZnO–Bi_2O_3–B_2O_3 glasses," *J. Non-Cryst. Solids,* **354** 5573–5579 (2008).
17. R. K. Mishra, V. Sudarsan, C. P. Kaushik, K. Raj, S. K. Kulshreshtha, and A. K. Tyagi, "Effect of BaO addition on the structural aspects and thermophysical

properties of sodium borosilicate glasses," *J. Non-Cryst. Solids,* **353** 1612–1617 (2007).

18. F. Lofaj, R. Satet, M. J. Hoffmann, and A. R. de Arellano López, "Thermal expansion and glass transition temperature of the rare-earth doped oxynitride glasses," *J. Eur. Ceram. Soc.*, **24** 3377-3385 (2004).
19. E-S. Lim, B-S. Kim, J-H. Lee, and J-J. Kim, "Characterization of the low temperature firing BaO-B_2O_3-SiO_2 glass: the effect of BaO content," *J. Eur. Ceram. Soc.*, **27** 825-829 (2007).
20. K. Gerth and C. Rüssel, "Crystallization of Bi_3TiNbO_9 from glasses in the system $Bi_2O_3/TiO_2/Nb_2O_5/B_2O_3/SiO_2$," *J. Non-Cryst. Solids,* **243** 52-60 (1999).
21. C. Rüssel and E. Freude, "Voltammetric studies of the redox behaviour of various multivalent ions in soda-lime-silica glass melts," *Phys. Chem. Glass,* **30** 62-68 (1989).
22. H. A. Silim, "Composition effect on some physical properties and FTIR spectra of alumino-borate glasses containing lithium, sodium, potassium and barium oxides," *Egypt. J. Solids,* **29** 293-302 (2006).
23. E. I. Kamitsos, M. A. Karakassides, and G. D. Chryssikos, "1. Vibrational spectra of magnesium-sodium-borate glasses. 2. Raman and mid-infrared investigation of the network structure," *J. Phys. Chem.,* **91** 1073-1079 (1987).
24. E. I. Kamitsos, A. P. Patsis, M. A. Karakassides, and G. D. Chryssikos, "Infrared reflectance spectra of lithium borate glasses," *J. Non-Cryst. Solids*, **126** 52-67 (1990).
25. B. D. Cullity, *Elements of X-Ray Diffraction,* 2nd edition, pp. 101–102. Addison-Wesley Publishing Co., London, 1978.

26. V. V. Golubkov, O. S. Dymshits, A. A. Zhilin, A. V. Redin, and M. P. Shepilov, "Crystallization of glasses in the K_2O–Nb_2O_5–SiO_2 system," *Glass Phys. Chem.,* **27** 504-511 (2001).

27. H. Tanaka, M. Yamamoto, Y. Takahashi, Y. Benino, T. Fujiwara, and T. Komatsu, "Crystalline phases and second harmonic intensities in potassium niobium silicate crystallized glasses," *Opt. Mater.,* **22** 71-79 (2003).

28. A. Aronne, V. N. Sigaev, P. Pernice, E. Fanelli, and L. Z. Usmanova, "Non-Isothermal crystallization and nanostructuring in potassium niobium silicate glasses," *J. Non-Cryst. Solids*, **337** 121-129 (2004).

29. P. Pernice, A. Aronne, V. N. Sigaev, P. D. Sarkisov, V. I. Molev, and S. Y. Stefanovich, "Crystallization behavior of potassium niobium silicate glasses. *J. Am. Ceram. Soc.,"* **82** 3447-3452 (1999).

30. P. Pernice, A. Aronne, V. N. Sigaev, and M. Kupriyanova, "Crystallization of the $K_2O \cdot Nb_2O_5 \cdot 2SiO_2$ glass: evidences for existence of bulk nanocrystalline structure," *J. Non-Cryst. Solids,* **275** 216-224 (2000).

Figure Captions

Fig. 1. Variation of density as a function of $BaBiBO_4$ content.

Fig. 2. Variation of refractive index of the glasses as a function of wavelength (for composition see Table I).

Fig. 3. DTA curves of B1 and B3b glasses (for composition see Table I).

Fig. 4. Linear thermal expansion curves of B1 and B4 glasses as a function of temperature. Their T_g, T_d and CTE values are also shown in the figure (for composition see Table I).

Fig. 5. Variation of T_g, T_d and T_s as a function of $BaBiBO_4$ content.

Fig. 6. Variation of coefficient of thermal expansion (CTE) as a function of $BaBiBO_4$ content.

Fig. 7. Vis-NIR transmission spectra of the B3a, B3b, B3c glasses melted at 1050, 1150 and 1250℃ respectively, and B4 glass melted at 1200℃ (for composition see Table I).

Fig. 8. FTIRR spectra of the glasses (for composition see Table I).

Fig. 9. XRD patterns of B3b glass and heat-treated B2 and B3b glasses at 580℃ for 2 h (for composition see Table I).

Fig. 10. (a), (b) and (c) FESEM images of surface crystallization, and (d) bulk crystallization of B3b glass-ceramics heat-treated at 580℃ for 2 h (for composition see Table I).

Fig. 11. (a) and (b) TEM images of B4 and B3c glasses melted at 1200 and 1250℃ respectively. (c) SAED and (d) HRTEM image of B3c glass melted at 1250℃ (for composition see Table I).

Fig. 12. Variation of dielectric constant as a function of $BaBiBO_4$ content.

Table I. Chemical Composition (Nominal), Melting Temperature and Color of Glasses

Sample identity	Composition (mol %)		Melting temperature (°C)	Color of glass
	$BaBiBO_4$[a]	SiO_2		
B1	90	10	1150	Yellow
B2	85	15	1150	Yellow
B3a	80	20	1050	Yellow
B3b	80	20	1150	Yellow
B3c	80	20	1250	Brown
B4	70	30	1200	Brown
B5	60	40	1200	Brown
B6	50	50	1200	Brown

[a] $BaBiBO_4$ = $50BaO\text{-}25Bi_2O_3\text{-}25B_2O_3$ (mol %)

Table II. Some Measured Properties of the Investigated Glasses

Glass identity [a]	B1	B2	B3	B4	B5	B6
Physical properties [b]						
M_{avg} (g. mol^{-1})	195.51	187.99	180.46	165.42	150.37	135.32
d ($g.cm^{-3}$)	6.1030	5.8870	5.8595	5.5915	5.1956	4.9301
V_M (cm^3)	32.035	31.933	30.797	29.584	28.942	27.447
Optical properties						
n_e (λ=546.1 nm)	1.96531	1.93196	1.92828	1.86897	1.82791	1.79460
n_F' (λ=480 nm)	1.98462	1.95471	1.94954	1.89979	1.83288	1.80722
n_C' (λ=643.8 nm)	1.94594	1.91157	1.90868	1.84905	1.81959	1.78199
R (%)	10.5972	10.1036	10.0492	9.17397	8.57107	8.08458
R_M (cm^3)	15.6417	15.2213	14.6402	13.4269	12.6861	11.6749
α (10^{-24} cm^3)	6.19985	6.03326	5.8029	5.3220	5.02838	4.62756

[a] For composition see Table I

[b] M_{avg} = average molecular weight, d = density, V_M = molar volume, ne, n_F', n_C' = refractive indices, R = reflection loss, R_M = molar refractivity and α = electronic polarizability

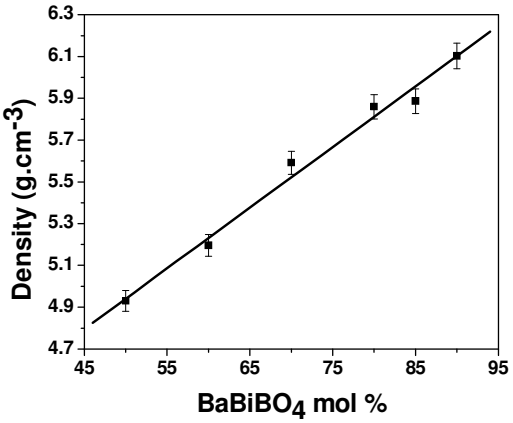

Fig. 1. Variation of density as a function of $BaBiBO_4$ content.

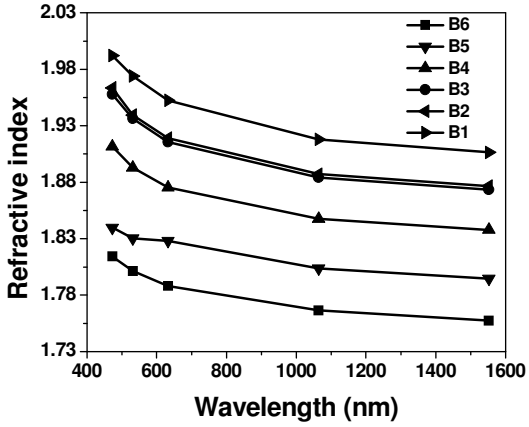

Fig. 2. Variation of refractive index of the glasses as a function of wavelength (for composition see Table I).

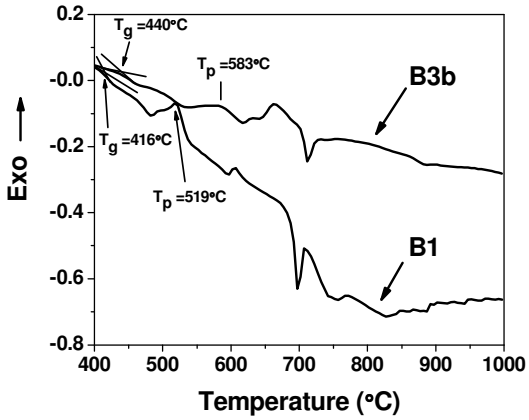

Fig. 3. DTA curves of B1 and B3b glasses (for composition see Table I).

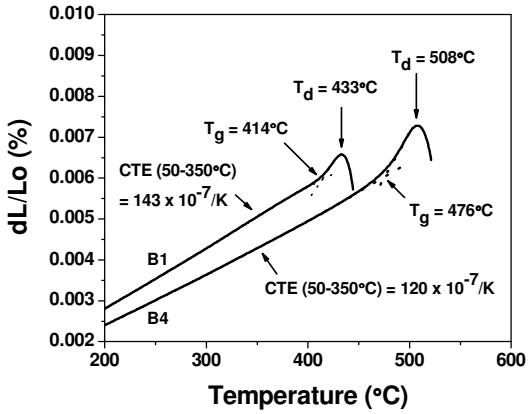

Fig. 4. Linear thermal expansion curves of B1 and B4 glasses as a function of temperature. Their T_g, T_d and CTE values are also shown in the figure (for composition see Table I).

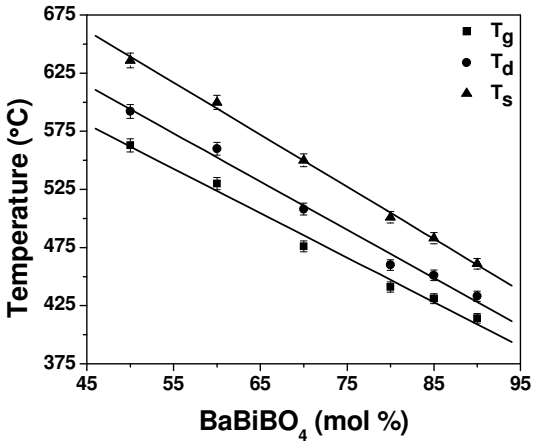

Fig. 5. Variation of T_g, T_d and T_s as a function of $BaBiBO_4$ content.

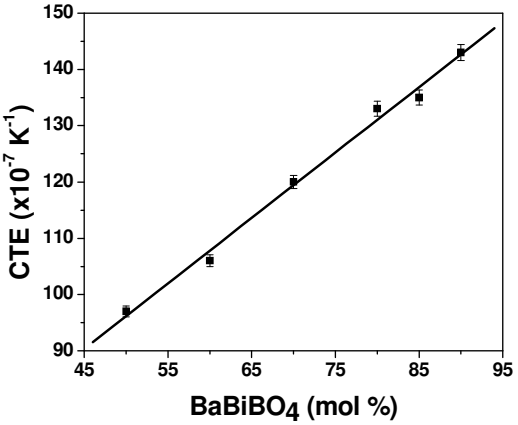

Fig. 6. Variation of coefficient of thermal expansion (CTE) as a function of $BaBiBO_4$ content.

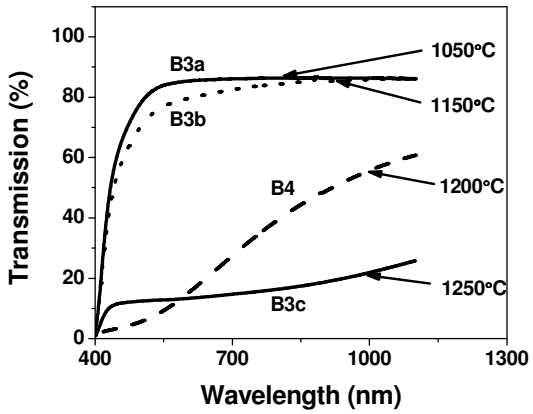

Fig. 7. Vis-NIR transmission spectra of the B3a, B3b, B3c glasses melted at 1050, 1150 and 1250℃ respectively, and B4 glass melted at 1200℃ (for composition see Table I).

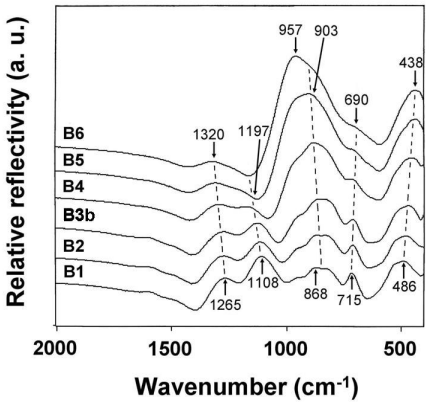

Fig. 8. FTIRR spectra of the glasses (for composition see Table I).

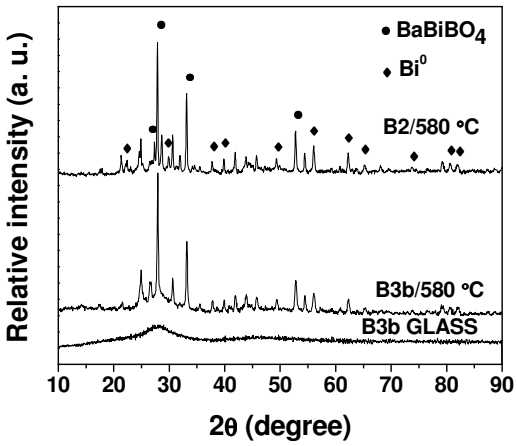

Fig. 9. XRD patterns of B3b glass and heat-treated B2 and B3b glasses at 580℃ for 2 h (for composition see Table I).

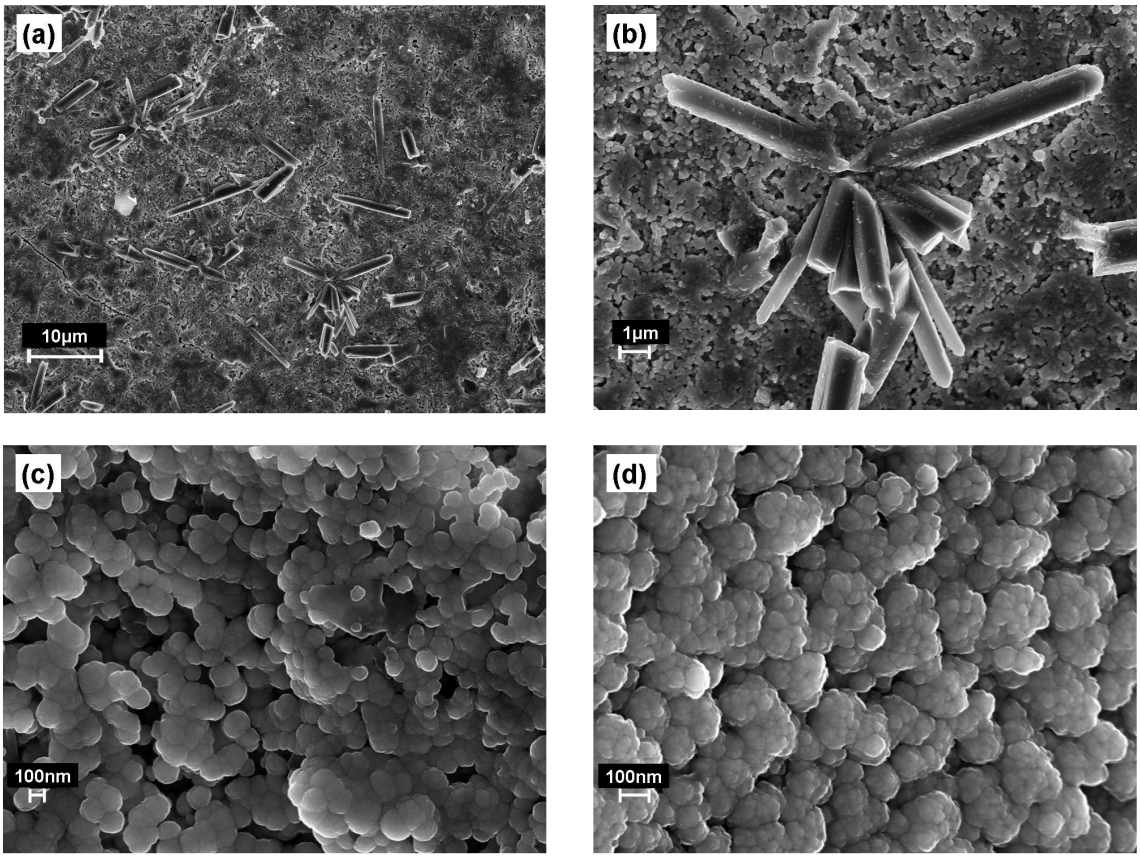

Fig. 10. (a), (b) and (c) FESEM images of surface crystallization, and (d) bulk crystallization of B3b glass-ceramics heat-treated at 580℃ for 2 h (for composition see Table I).

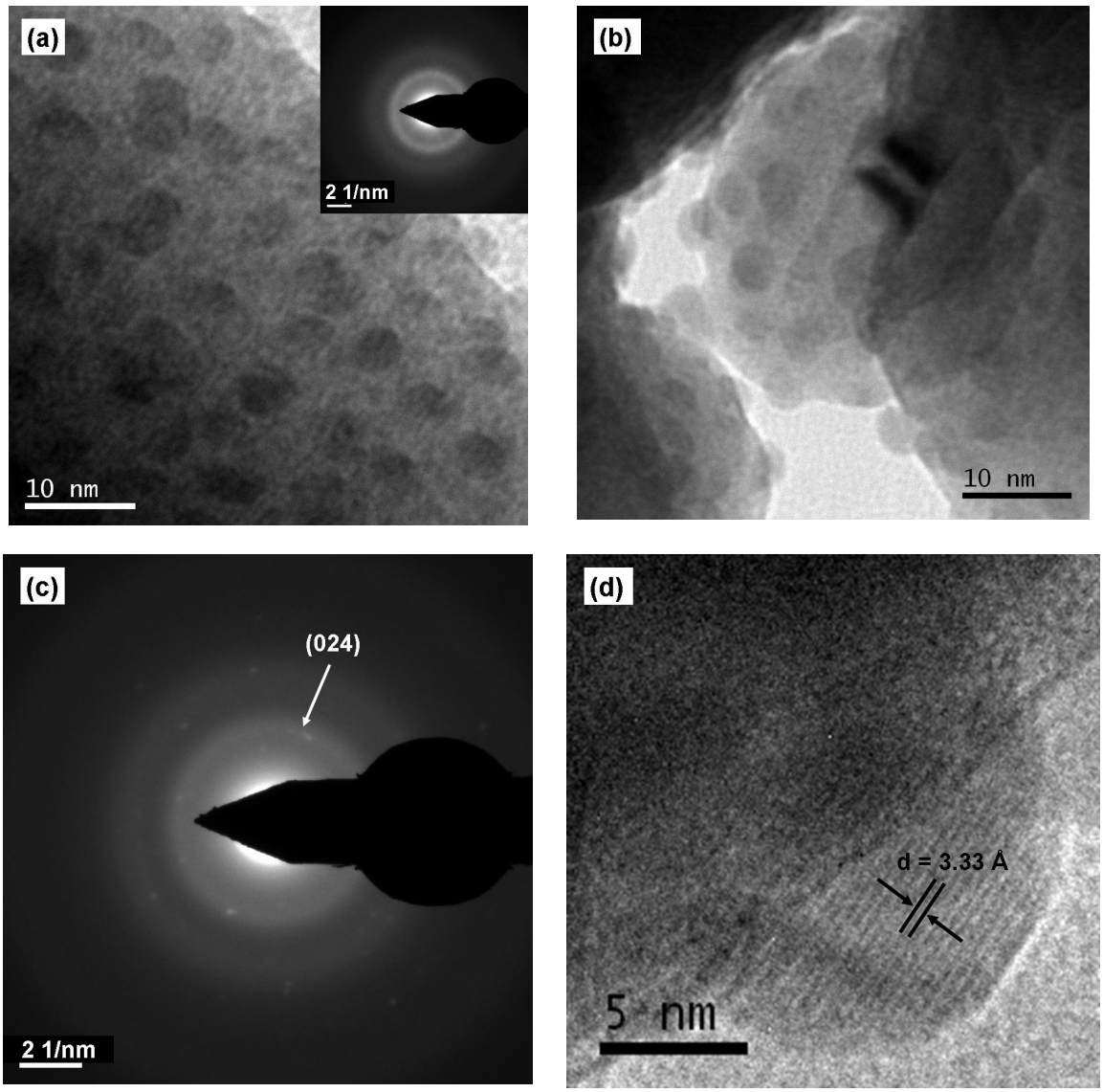

Fig. 11. (a) and (b) TEM images of B4 and B3c glasses melted at 1200 and 1250℃ respectively. (c) SAED and (d) HRTEM image of B3c glass melted at 1250℃ (for composition see Table I).

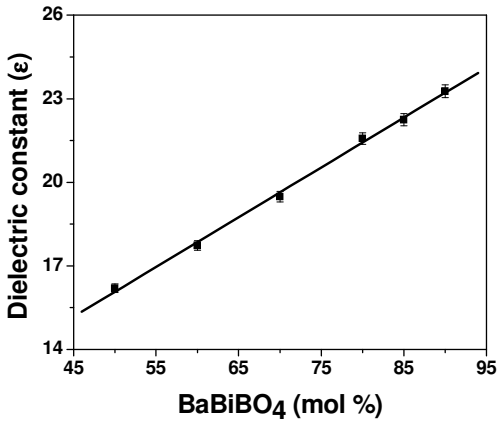

Fig. 12. Variation of dielectric constant as a function of $BaBiBO_4$ content.